

ESS
bilbao

Preliminary Design: MIRACLES Chopper System

Reference:	ESS-Bilbao
Date:	September 25, 2017
Revision:	1



Author	Review	Approved
P. Luna I. Herranz F. J. Villacorta	F. Sordo	J. L. Martinez



Contents

1	Introduction	4
2	New Concept	5
2.1	PWD chopper	6
2.2	PS chopper	7
2.2.1	Slit aperture selection for single PS disc	9
2.2.2	PS single disc performance for each operational mode	10
2.3	Operational modes: PWD and PS choppers	11
2.4	WBD/FO choppers	12
2.4.1	WBD/FO1 chopper disc	12
2.4.2	WBD/FO2 chopper disc	13
2.5	Wavelength at sample position	14

1 Introduction

Along with the design of MIRACLES' Backscattering Time of Flight Spectrometer, the neutron chopper cascade has to be set in order to transmit the desired wavelength range whilst providing the highest resolution achievable hence avoiding frame overlap. The instrument is facing the cold moderator, the complete chopper system is able to select a wavelength bandwidth of 1.6\AA centered within the range of neutron wavelengths from 2\AA to 20\AA . For scientific cases demanding elastic measurements for the Si-111 reflections the full chopper cascade can essentially be tuned to provide a wavelength band of 1.6\AA centered at 6.267\AA , however taking into account future Si-311 crystal upgrades on the second half of the analyser, the instrument could also allow for elastic measurements within a wavelength band of 1.6\AA centered at 3.27\AA (Si-311 reflection), as well as inelastic or QENS measurements.

All the studies included in this document are performed for elastic measurements with 6.27\AA (Si-111 reflection).

The main objective of this document is to come up with a solution in order to optimize the actual chopper system, while meeting with the instrument performance in terms of resolution and flux avoiding frame overlap. The first section of this document focuses on a chopper system description including 5 choppers (current chopper cascade) instead of the latest concept comprised of 6 chopper discs, arranged in 4 separate assemblies. The interest of this study was to check all modes of operation of the chopper cascade, hence the instrument performance. The possibility to work with one PS chopper is also considered, proving its viability.

A structural analysis is performed for each of the chopper discs of MIRACLES in order to check the viability of several materials which are currently used in the industry.

The first 5 chopper discs (first 3 chopper assemblies) have much stricter requirements since they will be placed inside the bunker, immediately after the monolith wall. Maintenance inside the bunker is limited to shut-down periods of the facility, for this reason, both disc and housing materials must be radiation resistant, therefore aluminium is considered for all chopper housings due to its fast decay.

The chopper cascade is comprised of 3 main disc types:

- PWD (Pulse Width Definition chopper): adapts flux vs. resolution, cutting the long pulse of ESS to improve the spectral resolution. This chopper provides the required time resolution.
- PS (Pulse Suppression chopper): selects a single pulse per source period.
- WBD/FO (Wavelength Band Definition/Frame Overlap chopper): selects the wavelength bandwidth, suppresses the harmonics transmitted by the PS chopper and prevents the frame overlap of subsequent pulses.

2 New Concept

This new chopper cascade concept is optimised in order to work with **5 chopper discs** along with the description of the different operational modes according to which choppers are properly tuned, looking carefully at every specific case to make sure the entire desired pulse is selected. This new concept is a reoptimization of the previous one, along with a analysis for each operational mode made disc by disc. Each case within the study has been carefully checked using the McStas tool.

Figure 1 represents an schematic view of the different chopper pits, the chopper assemblies and their position with respect to the moderator.

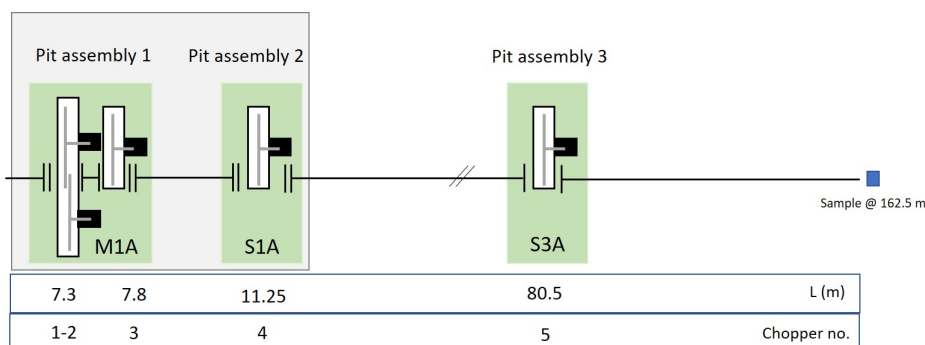


Figure 1: New chopper concept schematic layout: 5 axis

Table 1 summarizes the chopper cascade specifications and requirements for each of the chopper assemblies:

	Chopper assembly 1	Chopper Assembly 2	Chopper Assembly 3	Chopper Assembly 4
Function	PWD	PS	WBD/FO1	WBD/FO2
Position (m)	7.3	7.8	11.25	80.5
Type	Double disc CR	Single disc	Single disc	Single disc
Operating speed (Hz)	≤ 252	≤ 70	14	14
Disc material	CFRP	Aluminium 6061-T6	Aluminium 6061-T6	Aluminium 6061-T6
Disc diameter (mm)	700	700	700	700
Beam WxH (mm)	40x79	44x83	80x100	130x110
Depth of the window (mm)	83	87	104	114
Slit angle (°)	7.95° (x2) and 40° (x2)	28°	28°	167°
Arrangement	Over/Under	-	-	-
CHIM Variant	M1A chopper module, integrated guide		Pillar variant	Horizontal split
Absorber	B_4C enriched resin-epoxy	B_4C enriched resin-epoxy	B_4C enriched resin-epoxy	B_4C enriched resin-epoxy
Bearing type	Magnetic	Magnetic	Magnetic	Contact
Cooling	Yes	No	No	No

Table 1: Specifications and requirements of the chopper cascade

The vacuum level for the fast chopper pair is not defined yet, however it is expected for these choppers to work at a higher vacuum level than that for the guide. The first chopper pair needs cooling due to its high speed and its proximity to the moderator.

The performance of the complete chopper system is shown in the following Figure 2 which stands for the high resolution and high flux case.

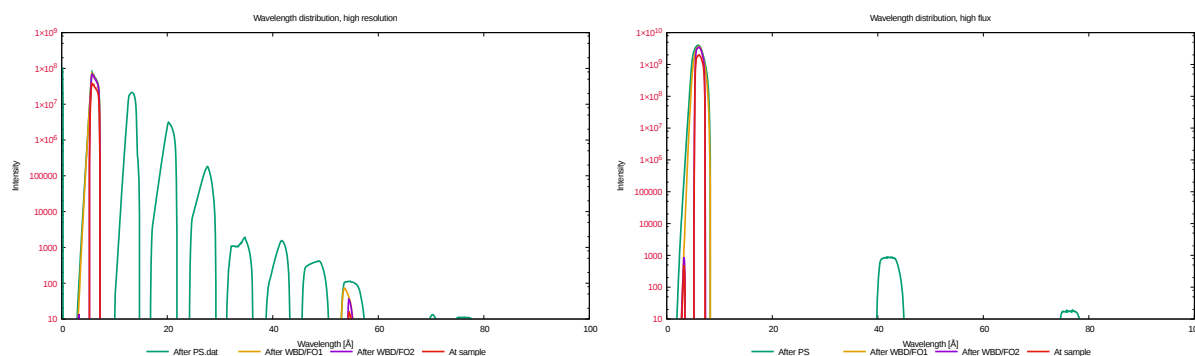


Figure 2: Wavelength distribution after each chopper assembly and reaching the sample, for the high resolution and high flux case.

According to this description, the costing estimation for the complete chopper system (based on [6]) is 934.5 k€, against the 1063.1 k€ Scope Setting meeting budget.

2.1 PWD chopper

The PWD counter rotating chopper pair has two main operational modes based on whether accounting for high flux or high resolution at sample. The chopper slit distribution from the proposal concept is preserved; both the 40° slits and the 7.95° slits, which are placed symmetrically in order to balance the chopper when rotating at its maximum speed of 252 Hz (15120 rpm).

The only modification of the PWD from the previous version is related to the double disc assembly. A **face-to-face configuration is being now considered for PWD double discs** despite the smaller distance existing between discs in an over-under configuration, about a 20 mm distance (with a face-to-face configuration the smallest distance is about 50 mm instead). However face-to-face provides a better stability when spinning at that high speed, therefore preventing the risk of failure.

The only concern about the present configuration is related to the proximity of the first disc motor with respect to the moderator, now placed upstream the guide. This fact implies the motor would receive higher radiation, what can end up heating up the motor.

On the other hand, the fact of placing the PS disc at 50 cm with respect to the previous chopper assembly might become an issue regarding possible interferences with the PS chopper module and housing, since the length for the magnetic bearing drives is 40 cm approximately.

A mechanical analysis has been carried out in order to select the most proper material for the PWD disc, details included in [1]. The study concludes CFRP discs present a good performance for an operational speed of 252 Hz, aluminium is definitely not a viable option for discs spinning

at that high speed.

2.2 PS chopper

Our new proposed concept allows for a single PS chopper disc instead of the previous concept consisting of double counter rotating chopper discs. The idea is to optimize the chopper cascade in order to work with 5 choppers while keeping the same performance when using single PS disc.

The disc will be set operate at a range of frequencies from 14 to 70 Hz whether accounting for high flux or high resolution. Figure 3 shows a comparison in time of flight between a single PS and a double PS disc:

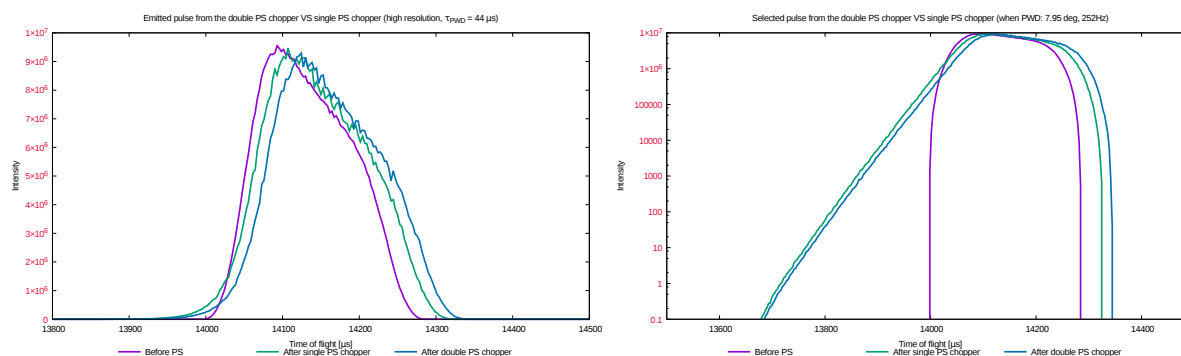


Figure 3: Comparison of the pulse filtered by the single PS disc and double PS discs, linear and logarithmic scale. The upcoming pulse shape is preserved. It is important to remark the placing of the monitors in the simulations is not the same after the single or double disc, thus the difference in time for each emitted pulse. The important thing to keep from this figures is the upcoming pulse is being preserved by the PS chopper

This implies a complete redesign of the PS disc needs to be carried out. First selecting an optimum slit aperture that allows the selection of the complete pulse coming from the PWD. This is first analysed for the high flux mode with choppers operating at their slowest speed. Once defining the slit aperture that works for high flux, the speed of the PS is increased until cheking the pulse for the high resolution mode is being properly selected, so the disc is expected to spin at its maximum speed.

The following figures 4 and 5 show the performance of the single PS disc in terms of wavelength distribution and time of flight.

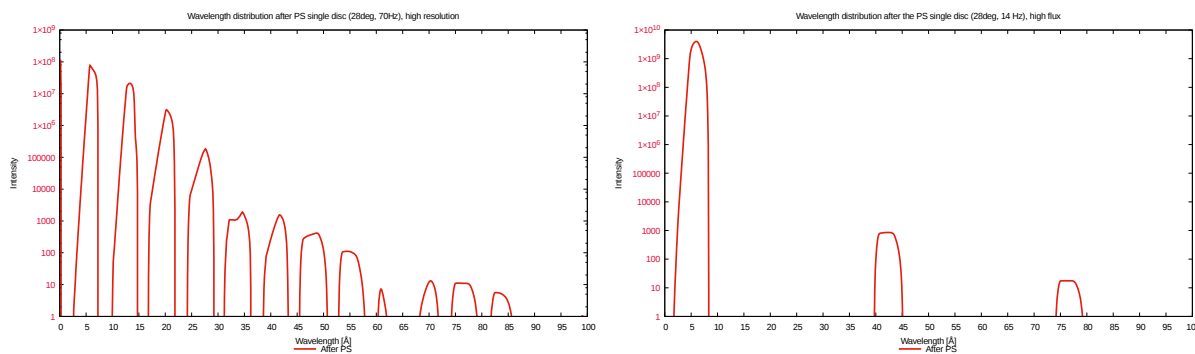


Figure 4: Wavelength distribution after the PS pair for both high resolution and high flux.

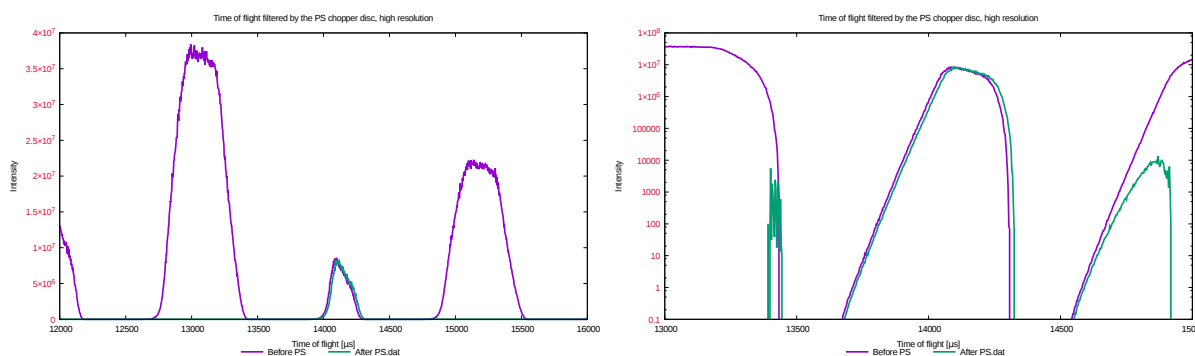


Figure 5: Comparison of the coming pulse from the PWD against the selected pulse by the PS single disc for **high resolution**. Linear and logarithmic scale

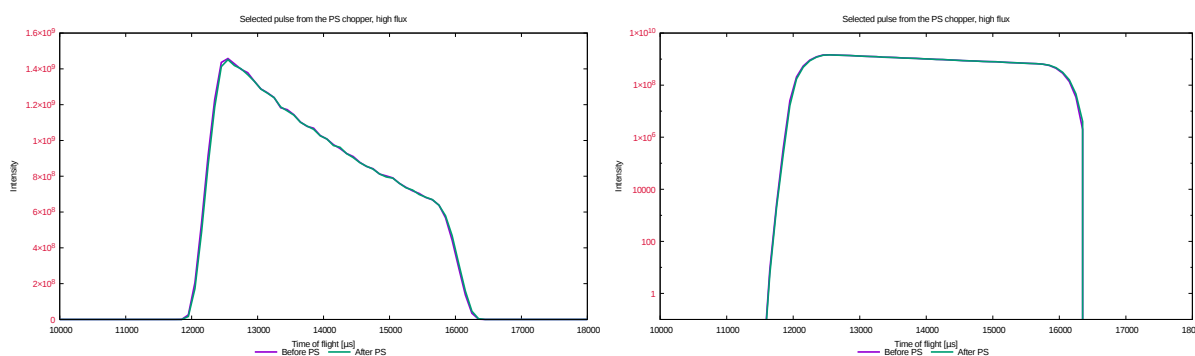


Figure 6: Comparison of the coming pulse from the PWD against the selected pulse by the PS single disc for **high flux**. Linear and logarithmic scale.

Aluminium alloy (6061-T6) is selected for the PS disc. Aluminium shows a good performance hence meeting the structural integrity of the disc. An structural analysis of the disc has been

carried out under the new PS conditions showing a peak stress value of 32.27 MPa concentrated at the edge of the axis.

2.2.1 Slit aperture selection for single PS disc

As the previous section states, results show a proper performance when selecting a single PS disc against the previous concept of the double disc. This section provides a detailed description of the analysis carried out in order to work with a single PS disc.

The PS chopper disc needs to allow the passage of a single pulse coming from the PWD accounting for each different operational mode of this chopper pair.

The starting point in the analysis of the PS slit angle selection is to consider the highest flux case, for which the **PWD is set at 28 Hz with 40° slits**. Based on these conditions the single PS disc is set at 14 Hz for which a wide range of slit angle apertures have been analysed in McStas (ranging from 5° to 120°).

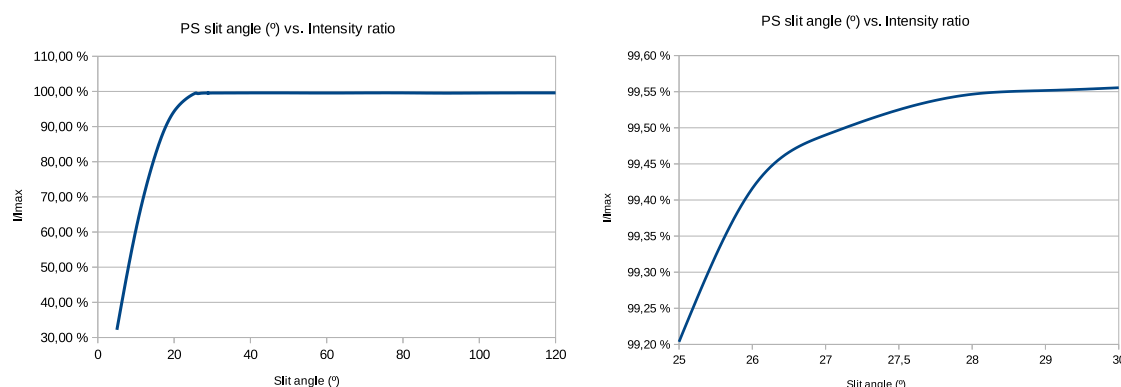


Figure 7: PS slit opening angles for a rotating frequency of 14 Hz

Figure 7 shows the different slit angles analysed against the percentage of the upcoming flux which is selected by the slit angles. Since PWD is set to operate in the high flux mode (40° and 28 Hz), the transmission through the PS disc (the flux passing through the disc against the flux that reaches the disc) has to be maximized when selecting the entire single pulse coming from the PWD. **The optimal slit angle for the PS chopper corresponds to 28°**, hence it has to account for the remaining intermediate operational modes of the PWD double disc (this can be achieved by only increasing the speed of the disc). As shown in Figure 8, the upcoming pulse is entirely selected by the PS disc for an slit angle of 28°.

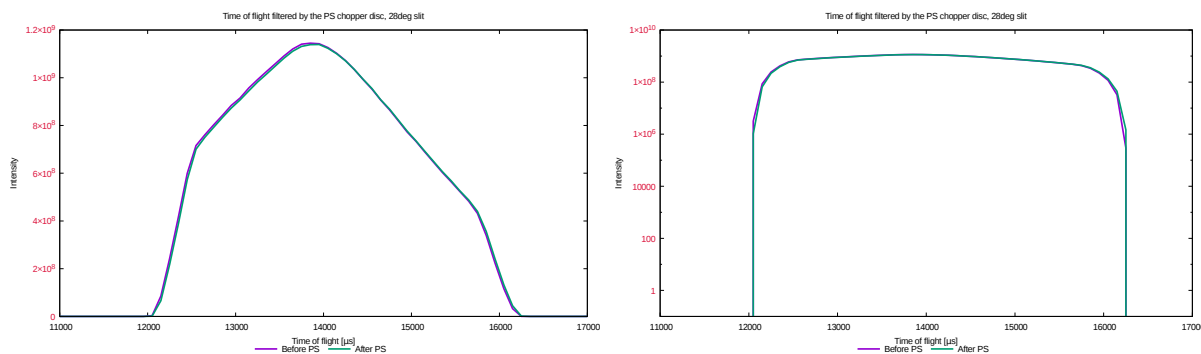


Figure 8: Pulse shape. Comparison of the pulse coming from the PWD against the pulse selected by the PS disc for a rotating frequency of 14 Hz. Linear and logarithmic scale

2.2.2 PS single disc performance for each operational mode

The performance of the instrument has to be studied according to the slit angle selected for the single PS disc, which has to be done by setting the PS disc rotational frequencies for each of the operational modes available for the instrument.

The following table shows the two main operational modes of the instrument, however other intermediate modes are also covered by the instrument but not included in this table:

PWD double disc			PS single disc	
Slit angle (°)	Frequency (Hz)	τ_{PWD} (ms)	Slit angle (°)	Frequency (Hz)
7.95°	252	0.044	28	70
	14	0.784	28	14
40°	252	0.22	28	70
	28	1.984	28	14

Table 2: Main operational modes of the chopper cascade

2.3 Operational modes: PWD and PS choppers

Modes of operation of the chopper cascade				
PWD Double Disc			PS Single Disc	
Slit angle (°)	Frequency (Hz)	τ_{PWD} (ms)	Slit angle (°)	Frequency (Hz)
7.95°	14	0.789	28	14
	28	0.394	28	14
	42	0.263	28	14
	56	0.197	28	14
	70	0.158	28	28
	84	0.131	28	28
	98	0.113	28	28
	112	0.099	28	56
	126	0.088	28	56
	140	0.079	28	56
	154	0.072	28	56
	168	0.066	28	56
	182	0.061	28	70
	196	0.056	28	70
	210	0.053	28	70
	224	0.049	28	70
	238	0.046	28	70
	252	0.044	28	70
40°	28	1.984	28	14
	42	1.323	28	14
	56	0.992	28	14
	70	0.794	28	14
	84	0.661	28	28
	98	0.567	28	28
	112	0.496	28	28
	126	0.441	28	28
	140	0.397	28	42
	154	0.361	28	42
	168	0.331	28	42
	182	0.305	28	56
	196	0.283	28	56
	210	0.265	28	56
	224	0.248	28	56
238	0.233	28	70	
	252	0.220	28	70

Table 3: Operational modes of the chopper cascade, highlighting both the **best resolution** and **high flux** modes.

2.4 WBD/FO choppers

The last 2 choppers of the instrument stand for the WBD/FO1 single chopper placed at 11.25m and the WBD/FO2 single chopper placed at 80.5m from the moderator. They are set to spin at 14 Hz whatever the operational mode of the instrument is. The operational modes of the WBD/FO1 and WBD/FO2 choppers for high flux and high resolution are shown in Table 4.

PWD double disc			PS double disc		WBD/FO1	WBD/FO2	Mode
Slit angle (°)	Frequency (Hz)	τ_{PWD} (ms)	Slit angle (°)	Frequency (Hz)	Frequency (Hz)	Frequency (Hz)	
7.95°	252	0.044	28	70	14	14	High resolution
40°	28	1.984	28	14	14	14	High flux

Table 4: Main operational modes of the current chopper cascade including WBD/FO choppers.

2.4.1 WBD/FO1 chopper disc

Based on the proposed concept, see [3], the WBD/FO1 is placed at a distance of 11.25m from the moderator, having a single slit aperture of 28°. Depending on whether accounting for high flux or high resolution the chopper disc is set to spin at 14 Hz for **suppressing all harmonics** transmitted by the PS chopper, hence the instrument is free of unwanted harmonics between 1-100Å.

In high flux mode, this chopper stops the second (42.49Å) and third (78.72Å) harmonics transmitted by the PS disc as shown in Figure 9.

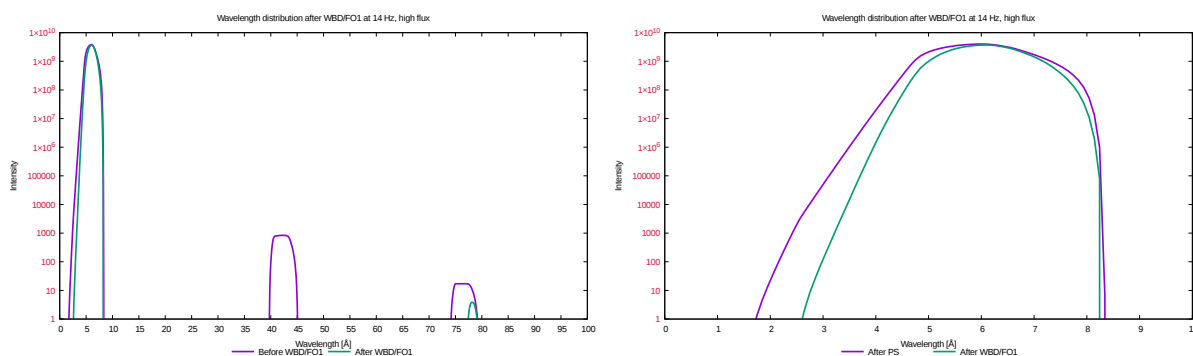


Figure 9: Wavelength distribution after WBD/FO1 spinning at 14 Hz, **high flux case**. Linear and logarithmic scale.

In case of high resolution, the WBD/FO1 disc is operating at 14 Hz stopping the following set of 6.27Å harmonics (for the elastic case) that reaches the WBD/FO1 as shown in Figure 10: first (13.51Å), second (20.76Å), third (28.00Å), fourth (35.25Å), fifth (42.49Å), sixth (49.74Å), seventh (56.98Å), eighth (64.23Å), ninth (71.48Å), tenth (78.72Å), eleventh (85.97Å) harmonics.

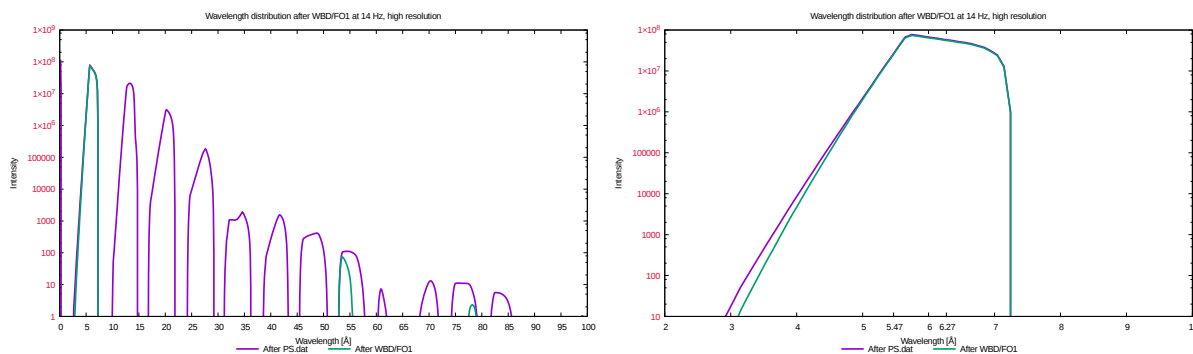


Figure 10: Wavelength distribution after WBD/FO1 spinning at 14 Hz, **best resolution** case.

2.4.2 WBD/FO2 chopper disc

Based on the proposed concept, see [3], the WBD/FO2 is placed at a distance of 80.5 m from the moderator, having a single slit aperture of 167° . For both high flux and best resolution cases the WBD/FO2 chopper disc is set to spin at 14 Hz therefore **selecting a wavelength bandwidth** of 1.6\AA of the upcoming pulse (from the WBD/FO1 chopper disc).

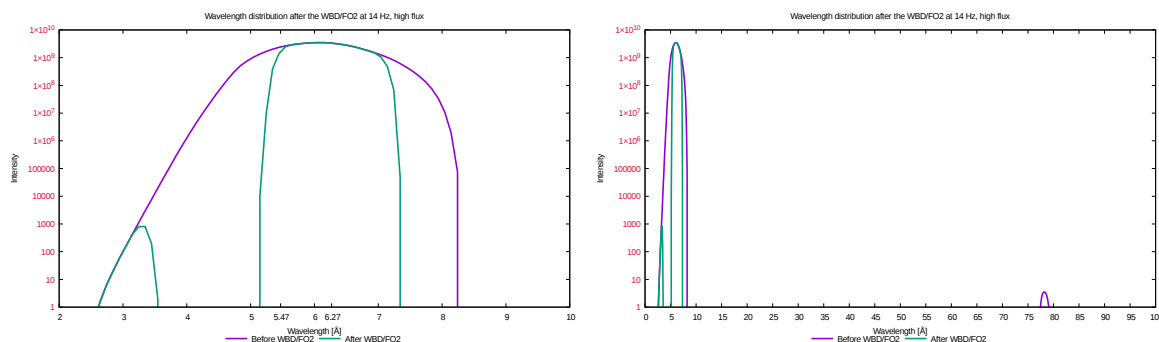


Figure 11: Wavelength distribution after WBD/FO2 spinning at 14 Hz, **high flux** case. Linear and logarithmic scale.

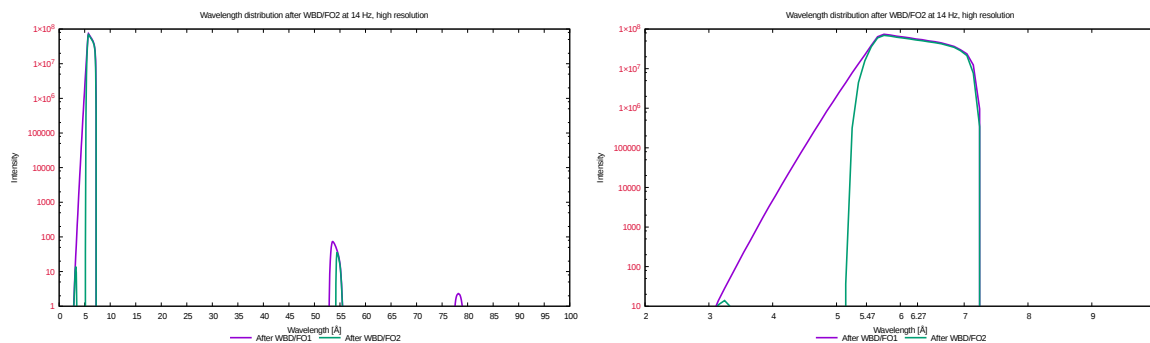


Figure 12: Wavelength distribution after WBD/FO2 spinning at 14 Hz, **best resolution** case.

2.5 Wavelength at sample position

The sample is placed at a distance of 162.5 m from the moderator, hence at 82 m from the final chopper (WBD/FO2). There is a loss in intensity arriving at sample as expected, what can be noticed in Figure 13, both for best resolution and high flux cases.

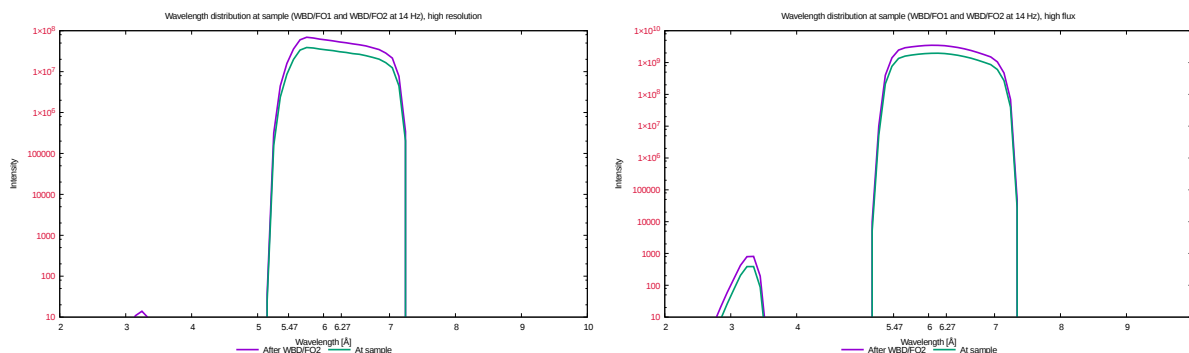


Figure 13: Wavelength distribution at sample, **best resolution and high flux** cases.

From the previous figure one can notice that for the **high flux case the intensity that reaches the sample is almost two orders of magnitude higher** than for the best resolution case.

Appendix 1: ESS Proposed Concept

By the end of March 2017, ESS suggested the MIRACLES team to consider an alternative chopper cascade concept that has been evaluated at ESS, which in fact is comprised by 4 choppers (against the new concept of 5 choppers).

Major changes (with respect to the 5 discs new concept) include a single PWD chopper spinning from 14 to 308 Hz and a single PS disc placed closer to the PWD (at 10 cm or even less) with a rotating frequency of 14 Hz. The following table includes the position, slit angle and rotating frequency of each chopper disc:

	Position (m)	opening (deg)	Frequency (Hz)
PWD	7.3	7.95	14-307
PS	7.4	12.31	14
BW/FO	17.9	37.67	14
BW/FO	87.6	184.4	14

Table 5: Configuration of the alternative chopper cascade proposed by ESS. [4].

This proposed chopper cascade concept represents a smart alternative solution for the chopper cascade, hence we have checked it carefully and conclude it almost meets the requirements of the instrument for highest flux and best resolution achievable. There are only small differences appreciable with respect to the 5 chopper concept which are discussed in the following subsections.

PWD chopper

Single PWD vs Double PWD

According to analytic calculations, a single disc rotating from 14 Hz to 308 Hz would correspond to a TOF-FWHM between 74 and 1629 μs , whereas a double disc rotating from 14 Hz to 252 Hz corresponds to a TOF-FWHM between 44 and 789 μs when using 7.95° and from 1984 μs and 220 μs when using 40° rotating from 28 to 252 Hz, respectively. By using the common equations, the best elastic resolution for a $3 \times 3 \text{ cm}^2$ sample (without changing any of the other influential parameters) would be 1.86 μeV in case of a double disc, and 2.08 μeV in case of a single disc.

Moreover, at the beginning of 2016 the MIRACLES team have studied the possibility of increasing the frequency of the first chopper, however we were suggested from ESS not to exceed 252 Hz, based on the fact that this chopper is placed inside the bunker, hence reducing the risk of disc failure. This is a must due to the low maintenance requirements inside the bunker.

When tuning for best resolution, double discs would actually provide a sharp pulse for such short cuts (44 μs for double disc) therefore enhancing the performance when best resolution is required.

The fact of using a counter-rotating pair provides a higher versatility, giving the option to place different slit angle apertures for different purposes, [9]. When compared to a double disc, the performance of a single disc is limited when accounting for two opposite goals (high flux and best resolution), since it only allows for one slit type working in both modes. Therefore, it will unavoidably have a worse performance in both high flux and best resolution when compared to double discs which allows for different slit apertures. It is not possible for a single disc to get the best performance in each case.

Comparison of both concepts

Several McStas simulations have been carried out in order to check the performance of this system with the respect to the one proposed in Section 2.

High flux

The maximum flux (within $6.267 \pm 0.8\text{\AA}$) Figure 14 shows a comparison of the selected pulse of the PS disc and the wavelength distribution at sample for both chopper systems in high flux mode. Single PWD disc spins at 14Hz with 7.95° slit against a double PWD spinning at 28Hz with 40° slit.

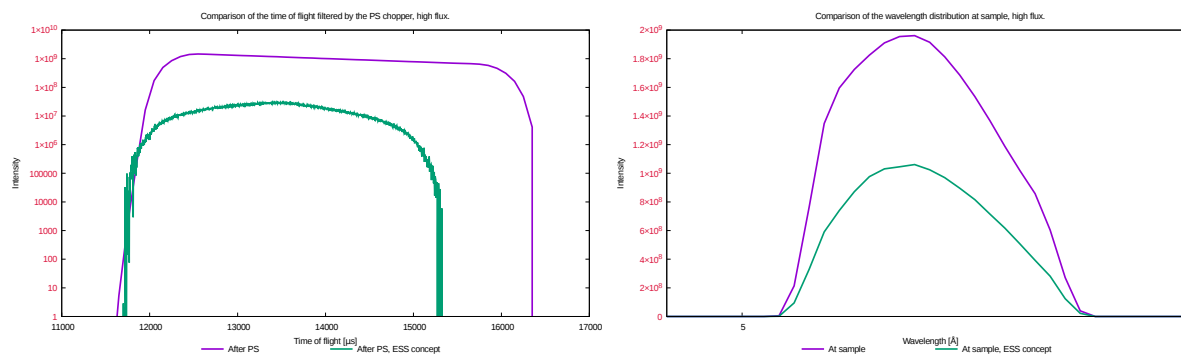


Figure 14: Comparison of the pulse shape after the PS chopper and wavelength distribution at sample between ESS concept and the concept proposed in 2.

According to McStas simulations the maximum intensity that reaches the sample for the ESS concept is $\approx 53\%$ of the intensity achieved with the 5 disc chopper cascade concept.

Best resolution

The time resolution of the primary spectrometer is a function of the opening time of the PWD chopper. Therefore in order to compare the time resolution it is necessary to define which is the opening time of the PWD chopper for both cases:

The opening time for the PWD chopper is obtained based on the following equations whether the PWD is comprised of a counter-rotating pair (1) or a single disc (2):

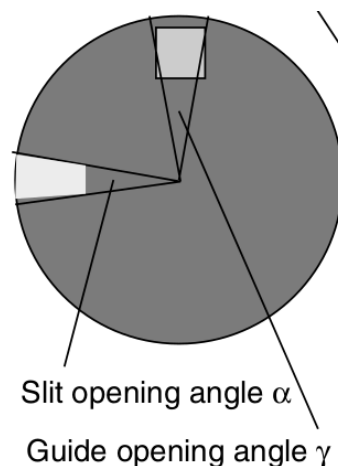
Double disc:

$$\tau_{PWD} = \frac{\alpha}{2 \cdot \omega} \quad (1)$$

Single disc:

$$\tau_{PWD} = \frac{\alpha + \gamma}{2 \cdot \omega} \quad (2)$$

τ stands for the opening time provided by the disc, as a function of the slit opening angle α , the angular speed of the disc ω and in the case of a single disc, the guide opening angle γ , as shown in Figure 2.5, [8].



For the highest resolution achievable, the opening time for each chopper system is **44 μ s** for the **new concept** and **74 μ s** for the **ESS concept**.

	Double CR	Single disc
α	7.95°	7.95°
ω	252 Hz	307 Hz
γ	-	8.48° (43mm x 120 mm guide)
τ_{PWD}	44μs	74μs

Based on the opening times, we conclude the best elastic resolution achievable for the ESS concept is **2.08 μ eV** while for the new chopper configuration the highest elastic resolution achievable is **1.86 μ eV**, both for a 3x3 cm^2 sample. It is a difference we might consider for the best resolution demanding scientific cases.

Windows along the beamline

It is important to be aware that reductions in flux will take place due to the placing of windows along the beamline. It is intended to use chopper windows only for choppers with integrated enclosure modules to be able to separate the different vacuum levels required at those chopper positions.

The chopper windows are not the only windows to be placed along the beamline, so it is highly important to minimize the total amount of aluminium for windows since the drawback of placing too many windows have a negative impact on the neutron transmission.[10].

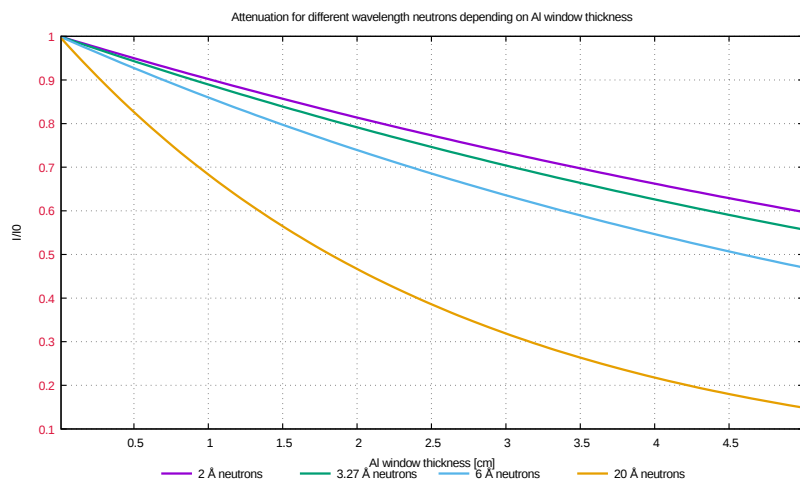


Figure 15: Attenuation for 2Å, 3.27Å, 6Å and 20Å neutrons depending on the aluminium window thickness

As one can tell from Figure 2, the neutron attenuation obtained when considering 4 windows of 5 mm thick represents 38% of losses at 6Å (wavelength of interest). There is a real need to limit the number of windows along the guide. The number of windows has to be limited to allow for the science case options which make use of a high neutron flux, since MIRACLES also characterized by its high flux.

Conclusions

The different chopper cascade options presented in this document have been analysed in order to find the best performance according to the scientific cases the instrument needs to cover. The chopper configuration that meets the best compromise between cost and performance will determine the option to go for. Two potential chopper configurations have been carefully evaluated, both 2 and 2.5, showing differences in performance. Perceptible differences between these two chopper cascades are related to the highest flux and best resolution achievable.

The ESS chopper system reaches less flux at sample with respect to the 5 chopper concept (2), meaning a 53% reduction in flux. We ought to reach the highest flux since reductions in flux will take place due to neutron absorption and scattering by the potential use of windows along the beamline, needed to isolate separate vacuum atmospheres.

With regards to the best resolution modes, we can conclude there is a slight difference when comparing both configurations. The 5 chopper disc system achieves a higher elastic resolution having a value of $1.86\mu\text{eV}$ when compared analytically against the $2.08\mu\text{eV}$ of the ESS chopper concept.

According to the structural analysis of the discs, results for aluminium alloy (6061-T6) show it is the most likely option in the case of slow speed choppers (PS pair, WBD/FO1 and WBD/FO2),



representing a chopper disc standardised design, what implies a reduction of the final costing with respect to other possible options. Fiber composite materials, specially the CFRP option seems to be the most suitable material when high speed chopper discs (PWD pair) are considered, showing a good performance on the selected discs.

Future works will focus on the optimization of the neutron absorber thickness applied on the whole outer ring of the disc as well as a further stress analysis including this absorber coating on the discs.

The fact of placing windows along the beamline has a high impact on the instrument performance highly penalizing the final flux reaching the sample, therefore we ought to select the chopper cascade that provides the highest flux.

The following table (Table 6) summarizes the requirements of the selected chopper cascade for MIRACLES:

	Chopper assembly 1	Chopper Assembly 2	Chopper Assembly 3	Chopper Assembly 4
Function	PWD	PS	WBD/FO1	WBD/FO2
Position (m)	7.3	7.8	11.25	80.5
Type	Double disc CR	Single disc	Single disc	Single disc
Operating speed (Hz):				
- High flux	28 Hz	14 Hz	14 Hz	14 Hz
- Best resolution	252 Hz	70 Hz	14 Hz	14 Hz
Disc material	CFRP	Aluminium 6061-T6	Aluminium 6061-T6	Aluminium 6061-T6
Disc diameter (mm)	700	700	700	700
Depth of the window (mm)	83	87	104	114
Slit angle (°)	7.95° (x2) and 40°(x2)	28°	28°	167°
Arrangement	Face-to-face	-	-	-
Best resolution case	$\tau_{PWD} = 44\mu s \rightarrow 1.86\mu eV$ for a $30 \times 30 \text{ mm}^2$ sample			

Table 6: Specifications and requirements of the chopper cascade

Appendix 2: Neutron Chopper Windows

Neutron absorption by aluminium windows

Aluminium windows are generally used due to its fast decay. In this section the aim is to evaluate which is the percentage of neutron losses when using aluminium windows along the beamline.

Results are shown in Table 2.5 for a single window of 5 mm thick.

Wavelength (Å)	Macroscopic cross section (cm^{-1})		I/I_{max} (%)		Intensity losses (%)	
	Absorption	Total (absorp.+ scatt.)	% due to absorption	% total (absorp. + scatt.)	due to absorption	due to abs.+ scatt.
2	0.016	0.103	99.22	94.96	0.78	5.04
3.27	0.026	0.117	98.73	94.33	1.27	5.67
6	0.047	0.151	97.68	92.75	2.32	7.25
20	0.157	0.381	92.47	82.65	7.53	17.35

Table 7: Percentage of neutron absorption and scattering for a 5mm thick aluminium window

Based on previous calculations, results in Figure 2.5 show the percentage of neutron attenuation obtained for different aluminium thicknesses. The impact of the window thickness is exponentially dependent on the neutron attenuation along the guide, therefore the total amount of aluminium to be placed along the beamline must be limited.

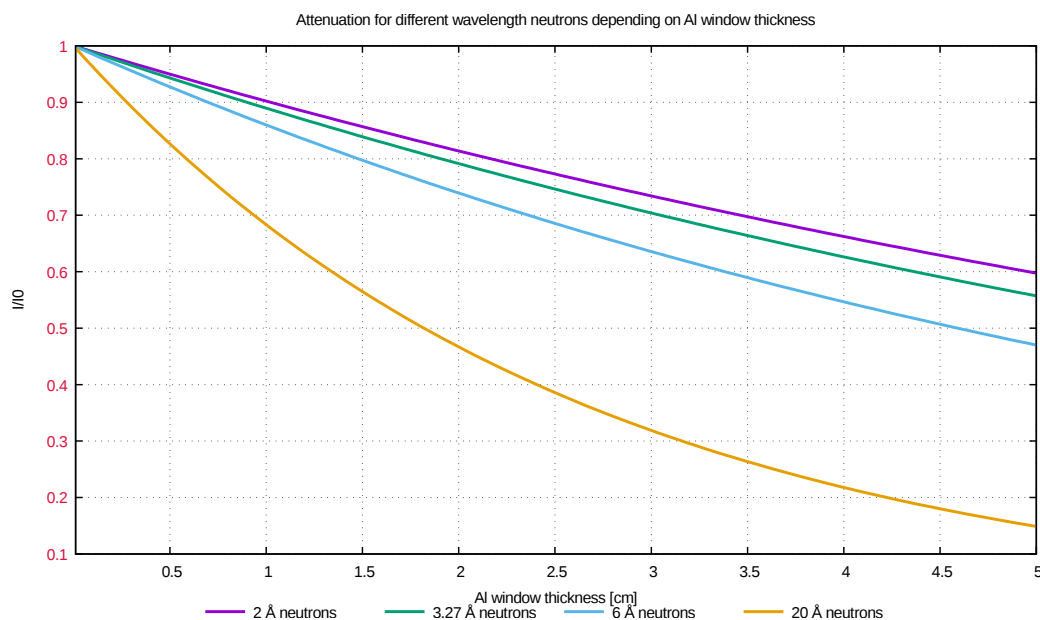


Figure 16: Attenuation for 2Å, 3.27Å, 6Å and 20Å neutrons depending on the aluminium window thickness.

As one can tell from Figure 2.5, the neutron attenuation obtained when considering 4 windows of 5 mm thick represents 38% of losses at 6Å (wavelength of interest). There is a real need to

limit the number of windows along the guide.

Structural analysis for the chopper windows

Possible windows for the different choppers in the cascade are (from smaller to larger dimensions):

- 40 x 120 mm^2 (WxH) window for the PWD chopper pit
- 43 x 120 mm^2 (WxH) window for the PS chopper pit
- 70 x 120 mm^2 (WxH) window for the WBD/FO1 chopper pit
- 120 x 120 mm^2 (WxH) window for the WBD/FO2 chopper pit

In this study only the smallest (40 x 120 mm^2) and largest windows (120 x 120 mm^2) are analysed. Each chopper assembly would have 2 windows; one at the entrance and one at the exit.

The following mechanical analysis for the chopper windows takes into account the **stress limit for Aluminium 6061-T6 is 87 MPa** (S_m) for membrane stress and **1.5x S_m** for both membrane and bending stress combined (the maximum stress against which results are compared is ≤ 87 MPa for membrane stress and $\leq 1.5 \times 87$ MPa = 130.5 MPa for the combined membrane + bending stress).

In the mechanical study a pressure of 1 bar is applied to the window face on one side, hence reaching the maximum stress right at the opposite face.

The following results show that the minimum **window thickness** to consider is **2mm** in both cases (40x120 mm^2 and 120x120 mm^2), so based on this, the neutron attenuation at 6Å would be 11.35% of the total flux for 4 windows (2.97% of neutron loss per 2mm window).

Window 4x12 cm^2 for the PWD chopper pair

In case of the PWD chopper it is most likely to include windows to allow for a separate vacuum between the guide and chopper atmosphere, since it will be mounted into an integrated enclosure chopper module therefore requiring 2 windows.

Two possible window geometries are considered: circular and rectangular, resulting smaller stress values in case of rectangular windows (having a smaller area).

Circular section window This circular window has a 6.45 cm radius, which is actually the equivalent circle to a 4x12 cm guide section. The following table (Table 8) includes the stress results for each window thickness (from 5 to 1 mm thick) considered in the analysis.

Window thickness (mm)	Stress at the center of the window (MPa)			Stress at the edge of the window (MPa)		
	Membrane (P_m)	Bending (P_b)	$P_m + P_b$	Membrane (P_m)	Bending (P_b)	$P_m + P_b$
5	1.18	10.01	11.13	1.47	8.48	9.18
4	1.46	14.38	15.84	1.93	14.27	15.28
3	1.91	21.03	25.95	2.56	27.37	28.67
2	2.60	51.89	54.49	3.79	64.82	66.90
1	4.19	202.12	206.39	12.26	261.62	272.27

Table 8: Stress values for each window thickness considered.

As shown in Table 8, stress values marked in red are actually exceeding the limit for aluminium. In fact a 1 mm thick aluminium window will actually break due to the combined membrane + bending stress. The bending stress is actually the major contributor to the total stress being concentrated at both central and external parts of the window.

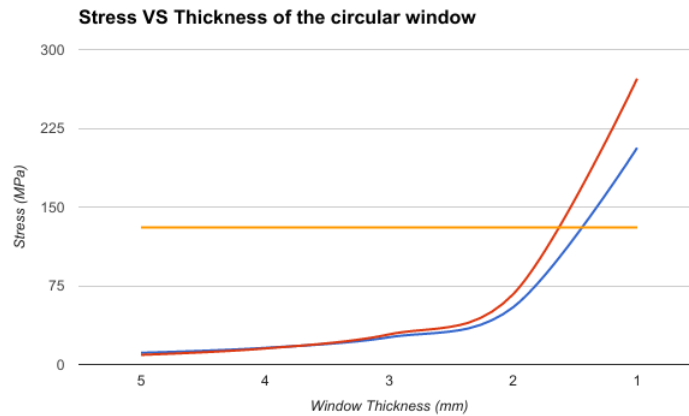


Figure 17: Maximum stress depending on window thickness.

Orange line stands for the aluminium limit of 130.5 MPa due to the combined membrane + bending stress. The **red line** represents the evolution of the maximum stress concentrated at the edge of the window while the **blue line** stands for the maximum stress concentrated at the center of the window, for each of the window thickness considered.

Therefore the minimum window thickness to consider in this case is the 2mm thick aluminium option. The stress and deformation distribution along this 2mm window is represented in Figure 18.

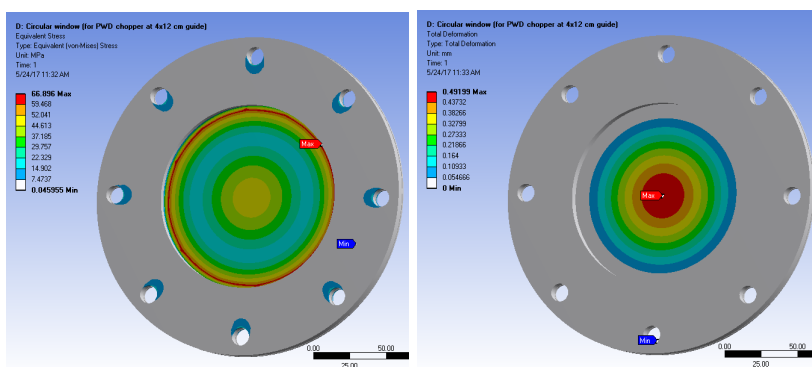


Figure 18: Stress and Deformation results along a 2mm thick aluminium window at a 40x120 mm^2 guide.

Rectangular window The following table includes the stress results for each window thickness (from 5 to 1 mm thick) considered in the analysis.

Window thickness (mm)	Stress at the center of the window (MPa)			Stress at the edge of the window (MPa)		
	Membrane (P_m)	Bending (P_b)	$P_m + P_b$	Membrane (P_m)	Bending (P_b)	$P_m + P_b$
5	1.03	4.04	5.07	1.32	1.00	3.27
4	1.42	4.65	6.06	1.19	1.51	4.04
3	1.93	6.28	8.18	1.09	2.18	5.97
2	2.72	11.54	14.21	3.43	11.48	13.57
1	4.37	41.05	42.43	8.44	50.19	56.74

Table 9: Stress values for each window thickness considered.

As shown in Table 8, in case of rectangular 4x12 cm^2 window, stress values do not exceed the limit for aluminium. Even a 1 mm thick aluminium window will theoretically withstand the pressure difference considered. Figure 19 actually represents the resulting stress values from Table 9 together with the maximum limit for aluminium 6061-T6 due to membrane + bending stress.

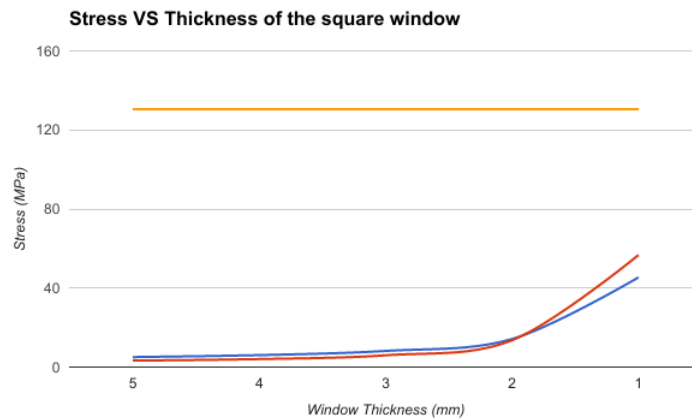


Figure 19: Maximum stress depending on window thickness.

Orange line: aluminium limit of 130.5 MPa due to the combined membrane + bending stress.
Red line: evolution of the maximum stress concentrated at the edge of the window for each window thickness. **Blue line:** maximum stress at the center of the window for each of the window thickness.

Depending on the window thickness, the maximum stress will be concentrated whether at the center of the window or at the edge.

In particular, for the smallest thickness the stress is maximum at the edge of the window, however when increasing the thickness of the window the maximum stress is concentrated at the center instead as shown in Figure 20.

However this maximum value is far below the aluminium limit of 87 MPa for membrane stress for each option as well as from the 130.5 MPa limit when considering the membrane plus bending effect.

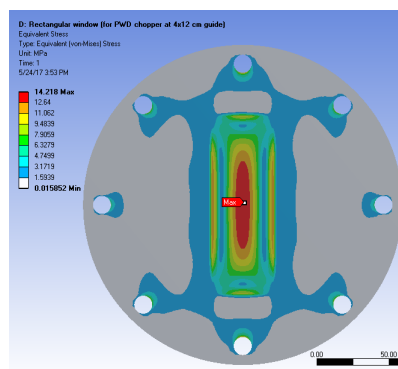


Figure 20: Stress distribution along the back face of a 2mm thick PWD chopper window at a $40 \times 120 \text{ mm}^2$ guide. The maximum stress value is concentrated at the center of the window.

Figure 21 represents the resulting stress and deformation distribution along the 2mm thick window.

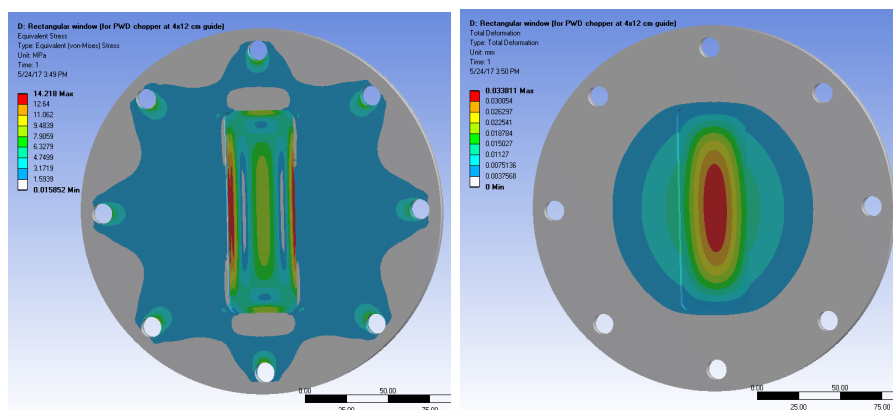


Figure 21: Stress and deformation results along a 2mm thick aluminium window at a $4 \times 12 \text{ cm}^2$ guide.

Window $12 \times 12 \text{ cm}^2$ for the WBD/FO2 chopper

Circular window This circular window has a radius of 8.49 cm, which is actually the equivalent circle to a $12 \times 12 \text{ cm}$ guide section. The following Table 10 gathers the maximum stress results obtained in the study for each window thickness considered, ranging from 5 to 1 mm thick.

Window thickness (mm)	Stress at the center of the window (MPa)			Stress at the edge of the window (MPa)		
	Membrane (P_m)	Bending (P_b)	$P_m + P_b$	Membrane (P_m)	Bending (P_b)	$P_m + P_b$
5	1.27	16.19	17.46			37.89
4	1.37	24.29	25.65			43.91
3	1.55	41.91	43.46	3.31	54.84	58.88
2	2.01	92.05	94.06	4.37	121.29	123.11
1	3.58	362.27	365.85	6.85	371.03	375.48

Table 10: Membrane and bending stress at the central part of the circular window and at the edge between the window and flange where the stress reaches the maximum value.

As shown in Table 10, stress values marked in red are actually exceeding the limit for aluminium. In fact a 1 mm thick aluminium window will actually break due to the combined membrane + bending stress. The bending stress is actually the major contributor to the total stress being concentrated at both central and external parts of the window. The window would actually break at its center and at the window-flange boundary.

For all window thickness options considered the resulting stress values at the window-flange boundary are higher than those at the central part, not exceeding the maximum value except for the 1mm window option.

Figure 22 represents the resulting stress values included in Table 10 together with the maximum stress limit for aluminium 6061-T6 of 130.5 MPa represented by the orange line.

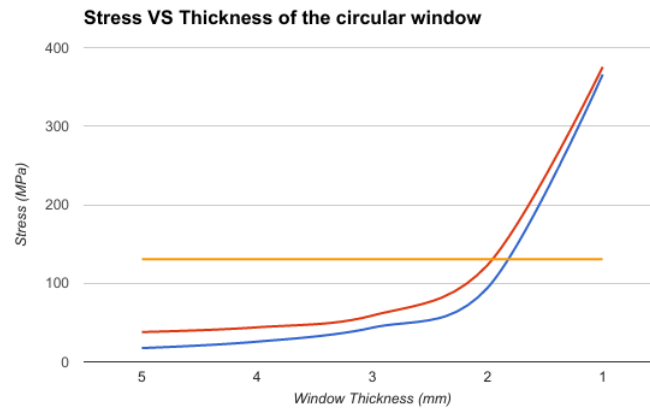


Figure 22: Maximum stress depending on window thickness.

Orange line: aluminium limit of 130.5 MPa due to the combined membrane + bending stress.
Red line: evolution of the maximum stress concentrated at the edge of the window for each window thickness.
Blue line: maximum stress at the center of the window for each of the window thickness.

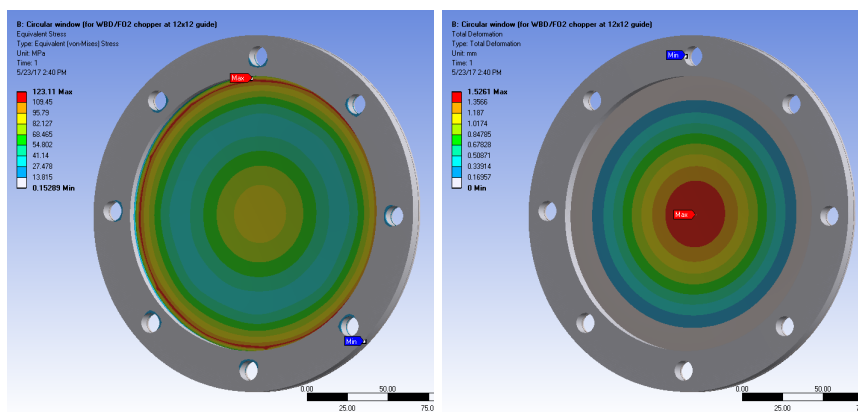


Figure 23: Stress and deformation results along a 2mm aluminium window at a 12x12cm² guide.

The minimum window thickness to consider in this case that would theoretically withstand that pressure difference -however being quite close to the maximum limit of 130.5 MPa at the window-flange boundary- is the 2mm option.

Rectangular window The following table includes the values of maximum stress for each window thickness (from 5 to 1 mm thick) considered in the analysis.

Window thickness (mm)	Stress at the center of the window (MPa)			Stress at the edge of the window (MPa)		
	Membrane (P_m)	Bending (P_b)	$P_m + P_b$	Membrane (P_m)	Bending (P_b)	$P_m + P_b$
5	1.08	10.78	11.85			11.71
4	1.43	15.40	16.83	2.90	18.22	21.12
3	1.89	25.57	27.46	4.26	35.11	19.37
2	2.60	54.76	57.36	6.48	84.74	89.74
1	4.20	212.50	216.70	12.98	350.88	360.06

Table 11: Membrane and bending stress at the central part of the $120 \times 120 \text{mm}^2$ window and at the edge between the window and flange where the stress reaches the maximum value.

Except for the 5mm window, the remainder options achieve their maximum stress at the window-flange boundary without reaching the limit for aluminium, except for the 1mm window which will inevitably break both at the boundary and the center of the window.

Figure 24 represent the stress values included in Table 2.5 together with the maximum limit for aluminium at 130.5 MPa.

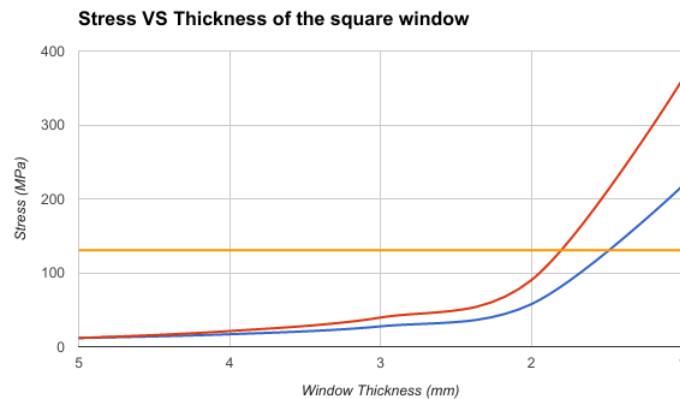


Figure 24: Maximum stress depending on window thickness.

Orange line: aluminium limit of 130.5 MPa due to the combined membrane + bending stress.
Red line: evolution of the maximum stress concentrated at the edge of the window for each window thickness.
Blue line: maximum stress at the center of the window for each of the window thickness.

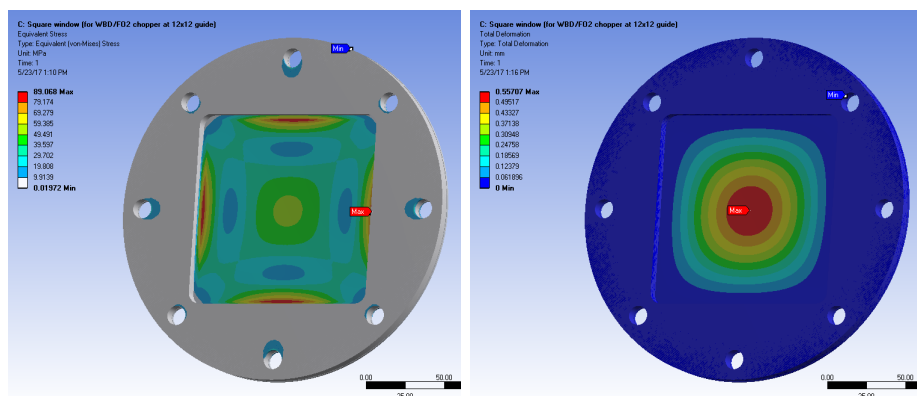


Figure 25: Stress and Deformation results along a 2mm aluminium window at a $12 \times 12 \text{ cm}^2$ guide.

In this case, the minimum window thickness that would theoretically work under that pressure difference is the 2mm option, for which the its maximum stress is far below the maximum limit for aluminium, as shown in Figure 25.

Conclusion

In this study, a structural analysis is performed for 2 different chopper window options; the PWD chopper window at a $40 \times 120 \text{ mm}^2$ guide and a WBD/FO2 chopper window at $120 \times 120 \text{ mm}^2$ guide, in order to check the minimum window thickness that could actually withstand the pressure difference existing at its position.

The optimization of the window thickness is of great importance since as shown in Section 2, neutrons will inevitably suffer absorption and scattering by any material (aluminium in this case) placed right in the middle of the beam path. The number of window have to be limited to allow for the science case options that make use of a high neutron flux, since MIRACLES is also characterized by its high flux. Aluminium is the material chosen for windows due to its fast decay.

Results show the most likely option to consider as the minimum thickness for the windows is 2mm. However it depends on the pressure difference existing at that position, which will probably will not be the same for all choppers that require windows. This study provides a general pressure difference for the possible window sections to be considered for the instrument.

Of course the dimensions of the windows have a huge impact on the final stress distribution. So what can be concluded in this analysis is that rectangular sections present a better behaviour under the same conditions than its equivalent circular window, which in comparison have a worse performance due to its larger area. In fact, the smaller the rectangular window is, the better to withstand the pressure difference existing at both faces.

References

- [1] *Miracles chopper discs: Structural Analysis*, ESS-Bilbao report, 2017.
- [2] P. Wang, B. Yang, W.L. Cai., *Development of a bandwidth limiting neutron chopper for CSNS*, Nuclear Instruments and Methods in Physics Research A, 2015.
- [3] *Redesign of the chopper cascade of MIRACLES in order to work with 6 choppers*, ESS-Bilbao report, 2016.
- [4] N. Tsapatsaris, *Report in optimized MIRACLES configuration*, European Spallation Source, 2017.
- [5] N. Tsapatsaris, R.E. Lechner, M. Markó and H. N. Bordallo, *Conceptual design of the time of flight backscattering spectrometer, MIRACLES, at the European Spallation Source*, Review of Scientific Instruments, 2016.
- [6] *Neutron Chopper Systems Costing Estimate, ESS-0060400*, ESS document, 2016.
- [7] Lechner RE. Physica B. 1992;180 and 181:973.
- [8] L. Liyuan, R. Rinaldi, H. Schober, *Chapter 3: Neutron scattering instrumentation (H. Schober)*, Neutron Applications in Earth, Energy and Environmental Sciences, 2009.
- [9] J. R. D. Copley, *Transmission properties of a counter-rotating pair of disk choppers*, Nuclear Instruments and Methods in Physics Research Section A, Volume 303, Issue 2, p. 332-341, 1991.
- [10] *Chopper windows: structural analysis*, ESS-Bilbao report, 2017.